Stem Cell Reports
Article

ISSCR

OPEN ACCESS

Direct Comparison of Four Hematopoietic Differentiation Methods from Human Induced Pluripotent Stem Cells

Melinda L. Tursky,[1,2] To Ha Loi,[1,2] Crisbel M. Artuz,[1] Suad Alateeq,[3] Ernst J. Wolvetang,[3] Helen Tao,[1,2] David D. Ma,[1,2,4,*] and Timothy J. Molloy[1,2,4,*]

[1]Blood, Stem Cell, and Cancer Research Programme, St Vincent's Centre for Applied Medical Research and Department of Hematology and BM Transplant, St Vincent's Hospital, Level 8, 405 Liverpool Street, Darlinghurst, NSW 2010, Australia
[2]St Vincent's Clinical School, Faculty of Medicine, UNSW Sydney, Sydney, NSW 2010, Australia
[3]Stem Cell Engineering Group, Australian Institute for Bioengineering and Nanotechnology, Brisbane, QLD 4072, Australia
[4]Co-senior author
*Correspondence: d.ma@amr.org.au (D.D.M.), t.molloy@amr.org.au (T.J.M.)
https://doi.org/10.1016/j.stemcr.2020.07.009

SUMMARY

Induced pluripotent stem cells (iPSCs) are an invaluable resource for the study of human disease. However, there are no standardized methods for differentiation into hematopoietic cells, and there is a lack of robust, direct comparisons of different methodologies. In the current study we improved a feeder-free, serum-free method for generation of hematopoietic cells from iPSCs, and directly compared this with three other commonly used strategies with respect to efficiency, repeatability, hands-on time, and cost. We also investigated their capability and sensitivity to model genetic hematopoietic disorders in cells derived from Down syndrome and β-thalassemia patients. Of these methods, a multistep monolayer-based method incorporating aryl hydrocarbon receptor hyperactivation ("2D-multistep") was the most efficient, generating significantly higher numbers of $CD34^+$ progenitor cells and functional hematopoietic progenitors, while being the most time- and cost-effective and most accurately recapitulating phenotypes of Down syndrome and β-thalassemia.

INTRODUCTION

Induced pluripotent stem cells (iPSCs) are an invaluable resource for the study of human disease and as a potentially limitless source of cells for therapeutic use. A plethora of methods for differentiation into a wide variety of cell types have been described (Liu et al., 2019). Published methods, however, display marked differences in culture additives, conditions, efficiencies, and cost, which affect both the practicality and reproducibility of target cell generation (Georgomanoli and Papapetrou, 2019). In addition, inconsistency in reporting and differences in laboratory practices make it difficult to draw comparisons across methods, hampering method selection to best answer specific biological questions. Direct comparisons of methods within a laboratory are therefore needed, yet there is a dearth of published direct comparisons of major differentiation methods.

The research and clinical value of patient-derived iPSC hematopoietic differentiation has been well demonstrated. Patient-derived iPSC lines have significantly contributed to our understanding of progression of malignant disorders and have been used for screening and identification of novel therapeutic compounds targeting specific mutations (Banno et al., 2016; Kotini et al., 2017). The establishment of good manufacturing practice protocols for iPSC generation and maintenance, and increasing use of iPSCs in clinical settings (Hansen et al., 2019), will ease translation of iPSC differentiation protocols into the clinic. The direct comparison of iPSC hematopoietic differentiation methods will contribute directly to progression of this field by identifying methods capable of producing large numbers of target cells, enabling standardization of protocols for particular endpoints, and creating work toward generation of clinically useful iPSC-derived cells. In addition, use of methods that are both serum-free and feeder-free will improve the clinical relevance of findings and expedite clinical translation (Liu et al., 2019).

To this end, we directly compared an optimized serum-free, feeder-free method with three other commonly used serum-free, feeder-free strategies utilizing a panel of iPSC lines, including assessment of efficiency, repeatability, and cost. In addition, we investigated the capability and sensitivity of these methods for modeling genetic hematopoietic disorders, such as recapitulation of proliferation and differentiation defects in cells derived from Down syndrome (DS) and β-thalassemia patients.

To represent the diversity of published methods for iPSC hematopoietic differentiation, we chose four common methods (Chou et al., 2012; Lapillonne et al., 2010; Niwa et al., 2011; Smith et al., 2013) that continue to be the basis of recent publications (Donada et al., 2019; Hansen et al., 2018; Leung et al., 2018; Wattanapanitch et al., 2018), two utilizing embryoid body (EB) three-dimensional (3D) formation, and two via monolayer two-dimensional (2D) culture. Within each culture system, one method with

few or "simple" culture stages and one based on a "multistep" differentiation strategy were selected.

We demonstrate that the optimized approach incorporating aryl hydrocarbon receptor (AhR) hyperactivation to drive hematopoietic stem/progenitor expansion combined improved efficiency with reduced hands-on time and cost, qualities important for large-scale research and therapeutic use. This optimized 2D-multistep method also showed the greatest utility and sensitivity in detecting the expected differences in hematopoietic progenitors from two patient groups with genetic defects leading to debilitating hematological diseases, namely DS and β-thalassemia.

RESULTS

Improvement of an iPSC Differentiation Method Incorporating 6-Formylindolo[3,2-b]Carbazole

A commonly cited method by Smith et al. (2013) demonstrated the value of AhR hyperactivation by 6-formylindolo[3,2-b]carbazole (FICZ) to stimulate the expansion of hematopoietic progenitor cells, particularly megakaryocyte-erythroid progenitors (MEPs), from iPSCs. However, this efficient culture system was associated with high cost. Our initial goal was to decrease the expense and hands-on time while improving hematopoietic cell-generation efficiency. In brief, optimization included omission of media changes on days 2, 3, 7, 10, and 15, and addition of reagents directly to culture wells on days 2, 7, and 10, thereby extending Wnt activation by 2 days and eliminating the day-3 increase in basic fibroblast growth factor (bFGF) concentration. This iteration of the 2D-multistep method (Table 1) resulted in more than 7-fold greater efficiency at generating $CD34^+$ progenitors, and $CD34^+CD45^+$ and $CD34^+CD43^+$ hematopoietic progenitors, while maintaining similar percentages of cells expressing or co-expressing erythroid $CD235a^+$ and/or megakaryocytic $CD41^+$ (Figure 1A) markers. In addition, the hands-on time required during culture from day 0 to harvest was reduced by 40%, and the overall cost of reagents per well was halved.

This method generated hematopoietic cells in suspension in increasing numbers from day 7, directly from the adherent iPSC-generated monolayer (Figures 1B and 1C), and was characterized by generation of 3D domed cellular structures arising from the monolayer from day 10 onward with cells visible at different focal planes (Figures 1D and 1E). Gentle harvest of suspension cells at day 16 caused disruption of these domes without visible disruption to the monolayer, suggesting that cells constituting these structures and/or from within these structures were present in subsequently harvested cells.

Functional hematopoietic progenitors, identified by colony-forming unit (CFU) assays (Figure S1), were present in suspension and adherent cell populations at similar frequency (per 1×10^6 $CD34^+$ cells), with production peaking at day 16 (Figure S2). However, the overall hematopoietic cell component of the adherent monolayer remained much lower than those in suspension (Figure S2). The generated suspension cells included a high proportion of $CD34^+$ progenitors that co-expressed cell-surface markers characteristic of multiple hematopoietic cell lineages (Figure 1F). For example, 41% of $CD34^+CD43^+$ hematopoietic progenitor cells co-expressed CD45 and CD235a (Figure 1G), which could be further subdivided into cells $CD33^+CD41a^-$ (20%), or $CD41a^+$ $CD33^{+/-}$ (80%) (Figure 1H). This cell population, combined with CD31 expression (Figure S2), is consistent with erythro-myeloid progenitor (EMP) potential (Garcia-Alegria et al., 2018). A distinct $CD34^+CD41a^+CD235a^+$ cell population was visible, identifying precursor erythrocyte-megakaryocyte cells (Belay et al., 2015) (Figure 1I). Analysis of $CD34^+$ $CD38^{+/-}$ cells identified subpopulations consistent with production of hematopoietic stem cells, multipotential progenitors, MEPs, and common myeloid progenitors (Mori et al., 2015) (Figure 1J). This is supported by the culture of day-16 suspension cells in CFU assays, which demonstrated robust colony formation with multilineage and lineage-specific progenitors including multipotent CFU-granulocyte-erythrocyte-monocyte-macrophage (CFU-GEMM), CFU–erythroid (CFU-E/BFU-E), CFU–myeloid (CFU-G/CFU-M, CFU-GM), and CFU–megakaryocytic (CFU-Mk) progenitors (Figure S1).

An Improved 2D-Multistep Approach Was the Most Efficient of Four Methods Compared for Generating Hematopoietic Cells from Human iPSCs

We directly compared this approach with three other representative serum- and feeder-free methods (Table 2): one additional monolayer method, and two via EB formation. Each method was characterized as "simple" or "multistep," depending on the number of sequential additive cocktails required for differentiation ("2D-multistep" optimized method, "2D-simple" [Niwa et al., 2011], "3D-multistep" [Chou et al., 2012], and "3D-simple" [Lapillonne et al., 2010]). Cells were harvested at the time point of maximal $CD34^+$ progenitor cell purity and/or CFU capability for each method. Of the four methods, the improved 2D-multistep strategy was most productive, producing the highest number of viable cells (10- to 13-fold higher than other methods; $p < 0.0001$; Figure 2A), highest percentages of viable $CD34^+$ progenitors (3-fold higher; $p < 0.0001$; Figure 2B), highest output of $CD34^+$ cells per 10^6 iPSCs (mean 4.7×10^5 per 10^6 iPSCs versus 7.2×10^4–3.8×10^5 per 10^6 IPCs; $p < 0.0001$; Figure 2C), and functional CFU per 10^6 iPSCs (mean 8.0×10^3 per 10^6 iPSC versus 3.8×10^2 to

Table 1. Comparison of Original and Improved 2D-Multistep Methods

	Day 0		1		2		3		4		5		6		7		8		9		10		11		12		13		14		15	
Reagent	A	B	A	B	A	B	A	B	A	B	A	B	A	B	A	B	A	B	A	B	A	B	A	B	A	B	A	B	A	B	A	B
RPMI (%)	95	95			95																											
KOSR (%)	5	5			5																											
StemPro (%)							100		100	100																						
IMDM (%)													74	74	74		+		+	+	+		+	+	+	+	+	+	+	+	+	
HAMS-F12 (%)													24	24	24		+		+	+	+		+	+	+	+	+	+	+	+	+	
N-2 supp (%)													0.5	0.5	0.5		+		+	+	+		+	+	+	+	+	+	+	+	+	
B-27 supp (%)													1	1	1		+		+	+	+		+	+	+	+	+	+	+	+	+	
BSA (%)													0.5	0.5	0.5		+		+	+	+		+	+	+	+	+	+	+	+	+	
MTG (mM)	0.4	0.4			0.4		0.4		0.4	0.4			0.4	0.4	0.4		+		+	+	+		+	+	+	+	+	+	+	+	+	
2PAA (mM)	0.3	0.3			0.3		0.3		0.3	0.3			0.3	0.3	0.3		+		+	+	+		+	+	+	+	+	+	+	+	+	
Wnt3a (ng/ml)	25	25																														
BMP4 (ng/ml)	5	5			5		5																									
VEGF (ng/ml)	50	50			50		50		15	15			50	50	50		+		+	+	+		+	+	+	+	+	+	+	+	+	
bFGF (ng/ml)					20	+20	50		5	5			100	100	100		+		+	+	+		+	+	+	+	+	+	+	+	+	
SCF (ng/ml)													100	100	100		+		+	+	+		+	+	+	+	+	+	+	+	+	
Flt3L (ng/ml)													25	25	25		+		+	+	+		+	+	+	+	+	+	+	+	+	
TPO (ng/ml)															50	+50	+		+	+	+		+	+	+	+	+	+	+	+	+	
IL6 (ng/ml)															10	+10	+		+	+	+		+	+	+	+	+	+	+	+	+	
EPO (U/ml)															0.5	+0.5	+		+	+	+		+	+	+	+	+	+	+	+	+	
FICZ (μM)															0.2	+0.2	+		+	+	+	+	+	+	+	+	+	+	+	+	+	
B differs from A	-		-		Add bFGF directly		No [high] bFGF		-		-		-		Add FICZ and cytokines directly		Fewer media top ups, add FICZ directly on day 10															

Direct comparison of media and additives and their final concentrations for the original Smith et al. (2013) (*A*, green) and the improved 2D-multistep (*B*, blue) methods. Values alone indicate a change of media, + followed by a number indicates this final concentration has been added to the existing media, and + alone indicates addition at the same concentration as added previously. The bottom row provides a summary of the changes made from the original protocol. 2PAA, 2-phospho-L-ascorbic acid; B-27 supp, B-27 supplement; bFGF, basic fibroblast growth factor ; BMP4, bone morphogenetic protein 4; BSA, bovine serum albumin; EPO, erythropoietin; FICZ, 6-formylindolo(3,2-*b*)carbazole; FLT3L, FMS-related tyrosine kinase 3 ligand; HAMS-F12, Ham's nutrient medium F-12; [high], high concentration; IL6, interleukin-6; IMDM, Iscove's modified Dulbecco's medium; KOSR, KnockOut Serum Replacement; MTG, monothioglycerol; N-2 supp, N-2 supplement; RPMI, Roswell Park Memorial Institute medium; SCF, stem cell factor; StemPro, StemPro-34 SFM Complete Medium; TPO, thrombopoietin; VEGF, vascular endothelial growth factor A165; Wnt3a, Wingless-type MMTV integration site 3A.

1.8×10^3 per 10^6 iPSCs; $p < 0.0001$; Figure 2D). No significant differences were observed in clonogenic potential of $CD34^+$ progenitor population produced by each method (Figure S3), indicating that the number of progenitors produced is affected, not their clonogenic potential. This supports a similar finding of human embryonic stem cell hematopoietic differentiation (Reid et al., 2018). The achieved clonogenic efficiency was high, with highest mean CFU/$CD34^+$ cells within an iPSC line of 1 in 19 $CD34^+$ cells forming CFU using the 2D-multistep method, while more than 20% of independent replicates showed more than 1 in 10 $CD34^+$ cells forming CFU (Figure S3). This high $CD34^+$ clonogenicity is comparable with the 1 in 10 achieved using a similar recent method (Lee et al., 2017).

A high degree of intra- and inter-iPSC line variability was observed when independent replicates of various iPSC lines were combined across methods (Figures 2A–2D and S3), consistent with reported findings (Kyttala et al., 2016). Analysis of data from two iPSC lines used to produce the largest proportion of data across all methods, analyzed individually or in combination across methods, gave results similar to those when independent replicates from multiple iPSC lines were combined (Figure S3; $p < 0.0001$ for live cells per 10^6 iPSCs, $CD34^+$ percentage and $CD34^+$ per 10^6 iPSCs; $p = 0.0002$ for CFU per 10^6 iPSCs), suggesting that combined data are not unbalanced by contributions from multiple iPSC lines.

A direct comparison of cell-surface markers was undertaken as a measure of hematopoietic progenitors and lineage potential. The 2D-multistep method proved the most efficient, with higher proportions of $CD235a^+$ cells (indicative of primitive or erythro/myeloid hematopoiesis and of erythroid-lineage cells), $CD45^+$ hematopoietic cells, $CD33^+$ myeloid cells, and $CD34^+$ progenitors co-expressing these markers (Figures 2E and S3; $p < 0.0001$ for all).

Methods were compared for hands-on time required to culture from day 0 to harvest and the relative cost.

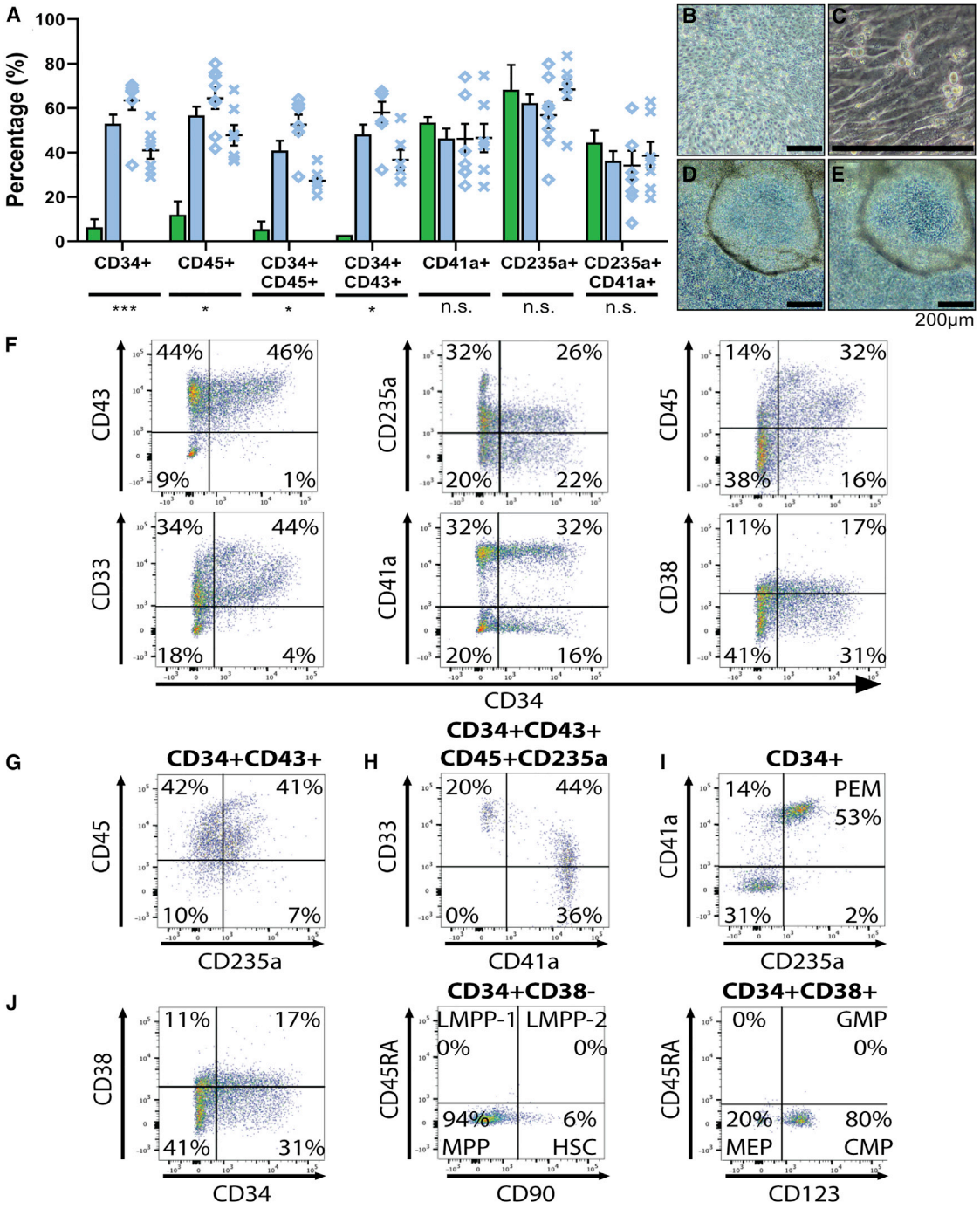

Figure 1. The Improved "2D-Multistep" iPSC Differentiation Method

(A) An iPSC differentiation method (green column) was improved, resulting in the 2D-multistep method (blue column) with more than 7-fold greater efficiency in producing hematopoietic progenitor cells. 2D-multistep data also shown as independent replicates from two iPSC lines (diamonds, n = 8; crosses, n = 7), with mean and standard error of the mean indicated. Statistical significance between columns was determined by t tests (*$p < 0.05$; ***$p < 0.001$; n.s., not significant).

(B–E) Representative light microscopy images during the 2D-multistep method, with monolayer giving rise to suspension cells from day 7 (bright cells in phase contrast) (B and C) and formation of 3D dome structures from day 10 containing cells visible on different focal planes (D and E). Scale bars, 200 μm.

(legend continued on next page)

Total hands-on time was calculated based on time required for media change or reagent addition per well, multiplied by number of wells required to produce 1 × 10^6 $CD34^+$ progenitor cells, and functional hematopoietic progenitor cells as assessed by CFU (Table S2). Relative cost was calculated from the volume of all reagents per well of culture and number of wells required to produce 1 × 10^6 $CD34^+$ progenitor cells and CFU, shown as cost and relative cost to the 2D-multistep method (Table 3). The 2D-multistep method was the most efficient in terms of hands-on time and cost for production of both $CD34^+$ progenitor cells and functional hematopoietic progenitors.

All Four Methods Produced Globin-Expressing Erythroid Cells Mimicking Embryonic Hematopoiesis

The production of mature globin-expressing erythroid cells is an important goal of iPSC research (Lapillonne et al., 2010). All methods generated globin-expressing cells with patterns reflective of yolk sac-derived EMP hematopoiesis (McGrath et al., 2011) (Figure 3A). Clinically relevant levels of β-globin were not observed in any method tested. Erythroid differentiation and maturation can be stimulated via use of erythropoietin (EPO), stem cell factor, dexamethasone, and/or insulin-like growth factor 1, with or without OP9 feeder cells; hence, we tested two methods for their effects on globin expression using 2D-multistep day-16 suspension cells. Harvested cells were either placed in Methocult CFU assays and BFU-E colonies picked after a further 16 days, or seeded onto OP9 feeder cells with erythroid differentiation additives and co-cultured for a further 17 days (Razaq et al., 2017) (Figures 3B and 3C). Both methods resulted in globin expression proportions similar to those of the improved 2D-multistep day-16 suspension cells (Figure 3D), suggesting that the CFU assay method is an efficient and simple way of producing erythroid cells and determining globin proportions, although neither method of erythroid differentiation resulted in β-globin expression equivalent to adult erythropoiesis. As globin-producing cells were already present in 2D-multistep day-16 suspension cells, these cells could be further cultured or enriched without use of feeder cells, which is an important consideration when generating cells for clinical use to minimize the possibility of therapeutic cell contamination.

The 2D-Multistep Method Successfully Recapitulated Key Features of Aberrant Hematopoiesis from DS- and β-Thalassemia-Derived iPSCs

We assessed the ability of each method to generate cells that recapitulate disease phenotypes using iPSCs derived from individuals with DS and β-thalassemia. Trisomy of chromosome 21 that characterizes DS induces acceleration of endothelial-to-hematopoietic transition during early hematopoiesis in iPSC-based models, with increased production of multi-, erythroid-, myeloid-, and megakaryocytic-lineage CFU (Banno et al., 2016; Chiang et al., 2018). Human fetal liver-derived hematopoiesis in DS individuals shows enhanced production of hematopoietic stem cells and MEP cells with a reduction in granulocyte-macrophage progenitor cells (Roy et al., 2012). Hematopoietic stem and progenitor cells (HSPCs) from DS individuals diagnosed with the highly prevalent, pre-malignant transient myeloproliferative disorder (TMD) triggered by mutation of *GATA1* display a strong proliferative phenotype with a myeloid bias (particularly megakaryocyte) at the expense of erythroid during differentiation both *in vitro* and *in vivo* (Banno et al., 2016). The proliferative phenotype and lineage bias of DS may therefore be dependent on the model used, developmental stage, and mutational landscape. Both the 2D-multistep and 3D-simple methods resulted in significantly increased total CFU per 10^6 $CD34^+$ cells derived from DS-iPSCs compared with wild-type (WT) iPSCs, consistent with the proliferative disease phenotype (Figure 4A; 3D-simple $p = 0.0255$; 2D-multistep $p = 0.001$). The increased total CFU observed with the 3D-simple method was characterized by increased numbers of multilineage and erythroid-lineage CFU in trisomy 21 DS cells (Figure S4; CFU-GEMM $p = 0.0014$; CFU-E/BFU-E $p = 0.0031$), indicating a lineage-specific proliferative phenotype. The 3D-simple, 3D-multistep, and 2D-simple methods demonstrated lineage bias from DS-iPSCs with increased proportions of total CFU being derived from the erythroid lineage (Figure 4B; $p < 0.0001$ for all). However, only the 2D-multistep method recapitulated the disease phenotype with increased clonogenicity observed for all CFU types in Methocult (Figure 4C; CFU-GEMM $p = 0.0029$; CFU-E/BFU-E $p = 0.0026$; CFU-GM $p = 0.0003$; total CFU $p = 0.001$) and Megacult (Figure 4D; $p = 0.0006$) assays, suggesting the erythroid-lineage bias detected by the other methods is only part of a multilineage proliferative phenotype that only the 2D-multistep method was sensitive

(F–J) Representative dot plots. (F) Suspension cells harvested on day 16 of the 2D-multistep method showing cell-surface expression and co-expression with CD34 progenitor cell marker. (G and H) A significant proportion of $CD34^+$ progenitors co-express markers indicative of several lineages. (I) A distinct $CD34^+CD41a^+CD235a^+$ precursor erythrocyte-megakaryocyte (PEM) cell population. (J) Analysis of the $CD34^+/CD38^{+/-}$ cells identified subpopulations consistent with production of hematopoietic stem cells (HSC), multipotential progenitors (MPP), megakaryocyte-erythroid progenitors (MEP), and common myeloid progenitors (CMP).
See also Figures S1 and S2; Table S1.

Table 2. Culture Conditions for the Four Methods Compared

	Day 0				2				4				6				7				9				10				11				12	13	14	15
Reagent	B	C	D	E	B	C	D	E	B	C	D	E	B	C	D	E	B	C	D	E	B	C	D	E	B	C	D	E	B	C	D	E	B	B	B	B
O2 (%)			5	5			5				5																									
RPMI (%)	95																																			
KOSR (%)	5																																			
StemPro (%)									100																											
IMDM (%)				97									74								+								+				+	+	+	
HAMS-F12 (%)													24								+								+				+	+	+	
SLII (%)		99	99				99			99	99			99																						
N-2 supp (%)													0.5								+								+				+	+	+	
B-27 supp (%)													1								+								+				+	+	+	
BSA (%)													0.5								+								+				+	+	+	
MTG (mM)	0.4								0.4				0.4								+								+				+	+	+	
2PAA (mM)	0.3								0.3				0.3								+								+				+	+	+	
ITS (%)		1	1				1			1	1			1																						
NHP (%)				3																																
Wnt3a (ng/ml)	25																																			
BMP4 (ng/ml)	5	20	25	10			25																													
VEGF (ng/ml)	50		50	5			50		15	40	50		50								+								+				+	+	+	
bFGF (ng/ml)					20		20		5		20		100								+								+				+	+	+	
SCF (ng/ml)				100			50			50	50		100	50							+								+				+	+	+	
Flt3L (ng/ml)				100			50				50		25								+								+				+	+	+	
TPO (ng/ml)				100			50				50			10			50				+								+				+	+	+	
IL6 (ng/ml)														50			10				+								+				+	+	+	
EPO (U/ml)														5			0.5				+								+				+	+	+	
IL3 (ng/ml)														50																						
FICZ (μM)																	0.2				+				+				+				+	+	+	

B (blue) = improved 2D-multistep, C (pink) = 2D-simple, D (yellow) = 3D-multistep, E (orange) = 3D-simple. Cells were harvested at the time point of maximal $CD34^+$ progenitor cell purity and/or colony-forming unit (CFU) capability for each method. Refer to Table 1 for explanation of + symbols and abbreviations. Additional abbreviations: IL3, interleukin-3; ITS, insulin transferrin-selenium; NHP, normal human plasma; O2, oxygen level; SLII, Stemline II hematopoietic stem cell expansion medium.

enough to detect. The data from various methods therefore recapitulated two phenotypes of DS-derived hematopoiesis previously reported in the literature, with increased numbers of CFU per 10^6 $CD34^+$ cells observed for all colony types, consistent with reports utilizing DS iPSC models (Banno et al., 2016; Chiang et al., 2018), and increased proportions of multilineage CFU-GEMM and erythroid-lineage CFU as well as a reduced proportion of granulocyte-macrophage progenitor cells, consistent with results utilizing DS-fetal liver-derived hematopoiesis (Roy et al., 2012). The iPSC lines used herein do not harbor the TMD-associated *GATA1* mutation.

We further demonstrated the ability of the 2D-multistep method to model genetic hematological diseases through the use of β-thalassemia-derived iPSCs. HSPCs from β-thalassemia patients show decreased erythroid differentiation efficiency (Finotti and Gambari, 2014). As expected, this method was sensitive enough to detect the decreased number of erythroid and total CFU (Figure 4E; CFU-E/BFU-E $p = 0.0497$; total CFU $p = 0.0436$). Together, these data suggest that the improved 2D-multistep method may be the most effective at recapitulating disease phenotypes and facilitating molecular and cellular characterization of iPSC-based genetic disease models.

DISCUSSION

Our results demonstrate that culture conditions can be optimized to produce EMP-like definitive hematopoietic progenitors with greater efficiency and reduced production time and cost while achieving precise disease modeling. In addition, direct comparison of this with three other serum-free and feeder-free iPSC hematopoietic differentiation

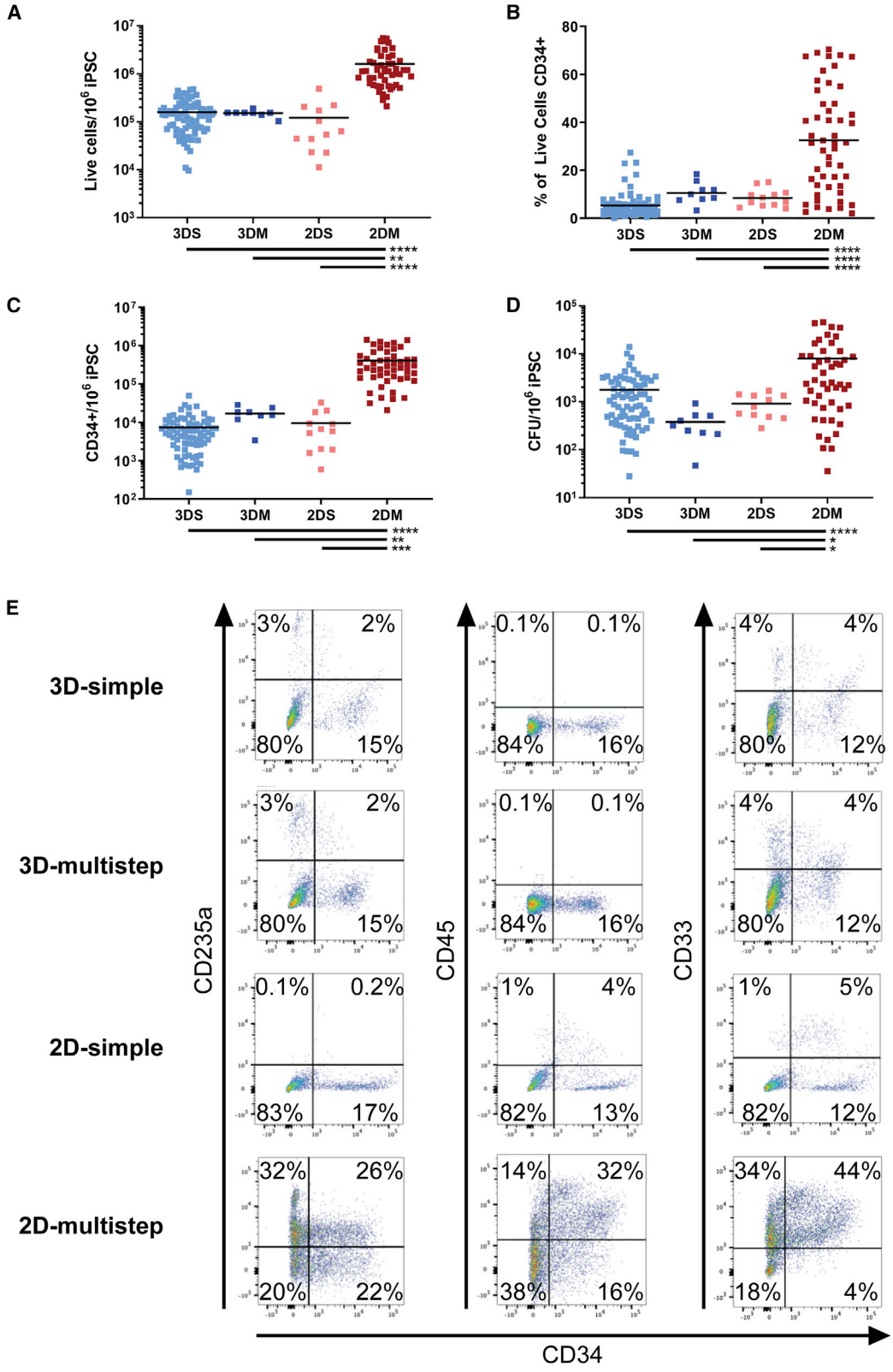

(legend on next page)

strategies fills an erstwhile unmet need for direct comparisons of iPSC hematopoietic culture systems.

We selected for improvement an efficient culture system that featured AhR activation. AhR has been hypothesized to be an important transcriptional regulator in several pathways of primitive or definitive hematopoietic development (as reported by us [Carlin et al., 2013] and others, reviewed in Angelos and Kaufman, 2018), with modulation of AhR through inhibition or hyperactivation having critical roles in HSPC emergence and proliferation, lineage commitment, and differentiation, including natural killer subtypes, T cells, monocytes, B cells, and macrophages. Smith et al. (2013) demonstrated that AhR hyperstimulation enhanced production of MEPs from iPSCs, with continual AhR stimulation inducing erythroid differentiation, with absence of AhR required for megakaryocytic differentiation. This is supported by other studies demonstrating that AhR inhibition of MEPs promotes both megakaryocytic differentiation and production of platelet-like elements (Angelos and Kaufman, 2018).

While the method of Smith et al. (2013) was efficient and tractable, it was relatively expensive. We performed systematic optimization of individual culture steps and used comparison with published data and kinetic analyses of cell phenotypes to produce an improved "2D-multistep" method, resulting in a 7-fold increase of $CD34^+$, $CD34^+CD45^+$, and $CD34^+CD43^+$ progenitors, while maintaining balanced production of $CD41^+$, $CD235a^+$, and $CD41^+CD235a^+$ erythroid and megakaryocytic cell populations as well as reducing hands-on time by 40% and halving the cost of reagents per well.

This improved method compared favorably with three other methods tested, producing ~3-fold greater proportion of viable $CD34^+$ progenitors, the highest output of $CD34^+$ cells and functional CFU per 10^6 iPSCs, and being the most efficient at producing hematopoietic progenitors and lineage committed cells. These findings confirm the value of AhR activation in the production of erythro-megakaryocytic progenitors. Interestingly, while the original AhR-derived hematopoietic differentiation method generated logarithmic expansion of suspension cells to day 20 (Smith et al., 2013), we observed ongoing expansion of $CD45^+$ hematopoietic cells, although HSPCs approached exhaustion around day 20, as assessed by flow cytometry and CFU assays, which is consistent with results reported by other groups (Angelos et al., 2017; Leung et al., 2018; Wattanapanitch et al., 2018). The choice of ligand, FICZ versus TCDD (2,3,7,8-tetrachlorodibenzo-p-dioxin), likely contributes to observed differences in AhR modulation during iPSC hematopoietic differentiation, as reported by others (Barouki et al., 2012).

Another important contributor to hematopoietic output is the developmental stage of hematopoiesis induced. Whereas *in vivo* hematopoiesis occurs in temporally and spatially distinct waves, sequentially characterized as primitive yolk sac, EMP, fetal, and bone marrow, iPSC hematopoietic differentiation does not delineate into such distinct developmental stages. In general, earlier protocols favored production of hematopoietic cells more reminiscent of primitive hematopoiesis, while recent methods incorporating modulation of Wnt activation and/or activin inhibition in early mesoderm formation produce cells characteristic of EMP and/or fetal liver hematopoiesis, which are transcriptionally, epigenetically, morphologically, and functionally more similar to adult hematopoiesis (Georgomanoli and Papapetrou, 2019).

In a study from the same laboratory, Leung et al. (2018) compared the original Smith et al. (2013) method with an HSPC-modified method that resulted in more robust production of hematopoietic progenitors, with more definitive-like erythroid CFU showing increased β-globin expression. Three-way comparison of the original 2D-multistep MEP protocol reported by Smith et al. (2013), the HSPC protocol reported by Leung et al. (2018), and the optimized 2D-multistep protocol presented herein showed that the HSPC and our 2D-multistep protocols shared important methodological differences from the original. These differences resulted in a shift toward EMP-definitive hematopoiesis, improved HSPC production efficiency, and more robust erythroid CFU colonies that expressed combinations of embryonic, fetal, and adult globins compared with the more primitive erythroid cells produced by the original MEP method (Leung et al., 2018; McGrath et al., 2011).

Figure 2. Direct Comparison of Four Methods of iPSC Hematopoietic Differentiation

(A) Comparison of the number of viable cells on the day of harvest, derived from 10^6 iPSCs seeded on day 0.

(B) Percentage of $CD34^+$ cells in the viable cell population.

(C) Number of $CD34^+$ cells derived from 10^6 iPSCs.

(D) Number of total CFU derived from 10^6 iPSCs.

(E) Representative dot plots showing hematopoietic differentiation efficiency was higher using the 2D-multistep method.

Each data point in (A) to (D) indicates an independent replicate (n = 8–77 replicates per group) from a variety of iPSC lines (n = 9 iPSC lines for 3D-simple, n = 6 iPSC lines for 3D-multistep and 2D-simple, n = 14 iPSC lines for 2D-multistep), with mean indicated by a horizontal line. Data were statistically significant by ordinary one-way ANOVA, with significance by post hoc Tukey's analysis shown below plots (all $p < 0.001$ by ANOVA; *$p < 0.05$; **$p < 0.01$, ***$p < 0.001$; ****$p < 0.0001$). See also Figure S3 and Table S2.

Table 3. Cost and Relative Cost of Each Method to Produce the Same Number of Target Cells

Output	2D-Multistep	2D-Simple	3D-Multistep	3D-Simple
Per 10^6 $CD34^+$ cells generated	$89 (relative cost = 1×)	$2,570 (29×)	$709 (8×)	$2,570 (29×)
Per 10^6 CFU generated	$5,230 (59×)	$14,182 (160×)	$69,848 (788×)	$10,637 (120×)

Calculations based on the 2018 list price and volume required for all reagents per well of culture, adjusted by the average numbers of $CD34^+$ cells and total colony-forming units (CFU) produced per method to determine the required number of wells to produce 1×10^6 of the target cells. Values in parentheses show cost relative to the 2D-multistep method for producing 1×10^6 $CD34^+$ cells stated as "relative cost = 1×," which equated to US$88.64.

Interestingly, while Smith et al. (2013) demonstrated AhR activation via FICZ-enhanced MEP production of ~3-fold by day 15 and a shift in differentiation to the erythroid lineage, Leung et al. (2018) observed contrary effects, reporting that the addition of FICZ during the HSPC protocol resulted in a ~3-fold reduction in hematopoietic progenitors on day 15 while AhR genetic knockout or inhibition resulted in a mild increase in hematopoietic progenitors. This suggests that AhR modulation is context dependent on protocol-induced differences. In comparison, our 2D-multistep method resulted in hematopoietic progenitors consistent with the HSPC protocol, yet with improved maintenance of hematopoietic progenitors cells by day 15 and greater clonogenic potential. Unlike the data presented by Leung et al. (2018), our data suggest that extended Wnt signaling promotes hematopoiesis characteristic of a more mature developmental stage that is compatible with FICZ-mediated AhR activation. The observed difference may be due to inherent variations in the HSPC methodology such as earlier introduction and higher concentration of thrombopoietin and interleukin-6 and absence of EPO. Future investigation through the use of Wnt and AhR modulators and multiple measures to distinguish primitive, EMP, and fetal liver developmental stages of hematopoiesis will help characterize the impact on progenitor production.

The methods used in this study were selected to represent the diversity of published methods on the strategy of hematopoietic induction. Other variations have been published. Minor modifications can induce earlier hematopoietic differentiation, such as Spin EB (Ng et al., 2008), and 2D-simple variants result in earlier and increased production of hematopoietic progenitors (Angelos et al., 2017; Hansen et al., 2018). However, the proportion of hematopoietic progenitors produced by flow cytometry or CFU remains lower than that obtained by the optimized 2D-multistep method. Methods containing 3D followed by 2D steps reportedly shift differentiation toward definitive-like hematopoiesis (Ditadi and Sturgeon, 2016) and enhance enucleation of red blood cells (Bernecker et al., 2019). However, these methods may be less cost- and/or time-effective than the 2D-multistep, as the former required a low oxygen environment and the latter required prolonged incubation, with definitive-like CFU appearing after day 21. Overall, the optimized 2D-multistep method resulted in the most efficient production of hematopoietic progenitor cells when directly compared with three other methods and with other published data, as indicated by the higher proportion of hematopoietic progenitors identified by flow cytometry, CFU assay, and lower hands-on time and cost to produce target numbers of these progenitors.

In this study variability was observed within and between iPSC lines during hematopoietic differentiation, as seen in other studies. Known factors that influence inter-iPSC variability include somatic epigenetic memory and genetic diversity of the originating cell, and genetic and epigenetic aberrations introduced during reprogramming (Kyttala et al., 2016; Nishizawa et al., 2016; Salomonis et al., 2016). The main contributor to intra-iPSC line variability is the inherent complexity of hematopoietic differentiation, as at no stage of the differentiation process is the cell population homogeneous. This, combined with technical caveats such as manual handling and differences between reagents, results in small differences in the initial cell population composition magnified through differentiation to culture endpoints. As iPSC hematopoietic differentiation protocols are refined, heterogeneity of cell populations will reduce, thereby reducing variability (Papapetrou, 2019).

Patient-derived iPSCs are important models of disease due to their derivation from human tissue and amenability to genome engineering. This paradigm has facilitated the study of genetic diseases such as DS, characterized by the presence of an additional copy of chromosome 21, and β-thalassemia, characterized by mutations in the *HBB* gene. DS has multisystem effects such as neuronal and cardiac defects, in addition to abnormalities in erythrocytosis, thrombocytopenia, and leukocytosis, and a markedly increased risk of TMD and leukemia (Roy et al., 2009). β-Thalassemia leads to deficiency in β-globin synthesis and is associated with ineffective erythropoiesis (Finotti and Gambari, 2014). Similar to other genetic diseases, DS and β-thalassemia during embryogenesis have been difficult to study due to ethical limitations, and animal models are imperfect avatars. Patient-derived iPSC-based disease models provide an important alternative. The enhanced expansion of erythro-megakaryocytic lineages from DS-derived iPSCs resembled EMP-like hematopoiesis in this study, suggesting that these effects may be initiated in DS

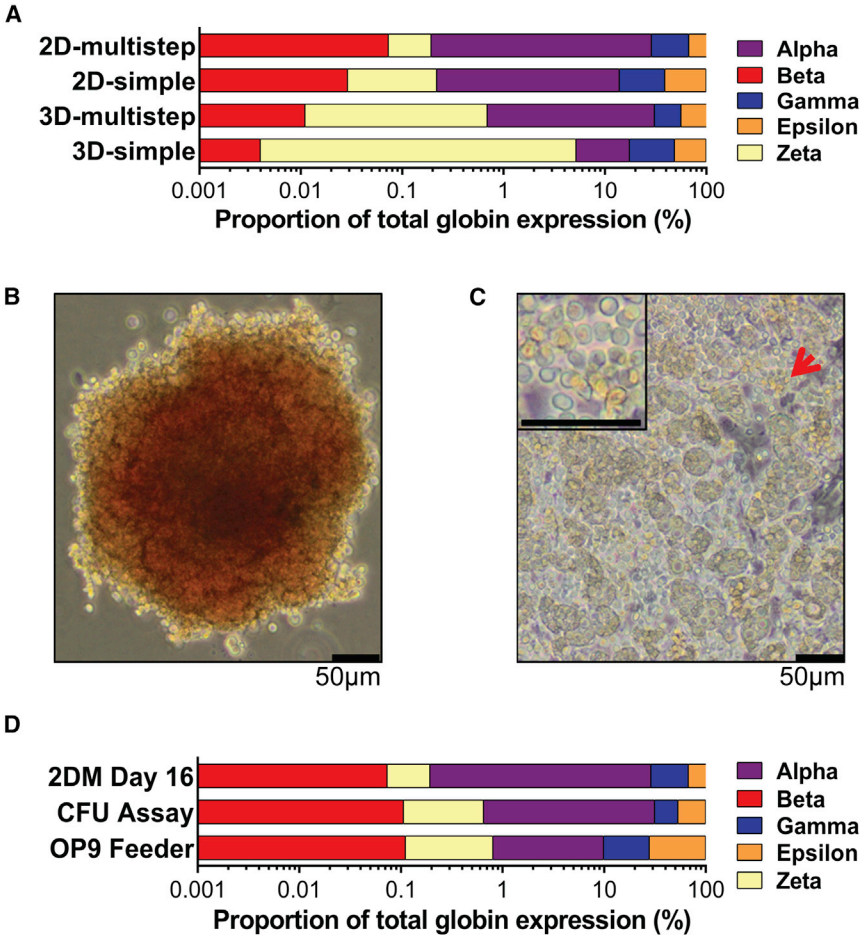

Figure 3. Globin Production Using Four Methods of iPSC Hematopoietic Differentiation

(A) Representative data of the four methods showing relative proportion of total globin expression (measured by qPCR).

(B and C) Following 16 days of hematopoietic differentiation, 2D-multistep suspension cells were further cultured by one of two methods to induce erythroid differentiation. Representative BFU-E formed after a further 16 days of culture in Methocult Enriched medium (B), and individual round hematopoietic cells (red arrow and inset image) expanded on OP9 feeder cells after a further 17 days of culture (C). Scale bars, 50 μm.

(D) Representative data of the relative proportion of total globin expression following CFU assay and OP9 feeder cell-based cultures compared with the originating 2D-multistep (2DM) day-16 harvested cells.

See also Table S3.

during early development. The 2D-multistep method was most sensitive in recapitulating the disease phenotype, with increased clonogenicity observed for all CFU types. iPSCs derived from β-thalassemia patients similarly displayed decreased erythropoiesis using the 2D-multistep method, consistent with the expected disease phenotype.

A potential role for iPSCs is the large-scale production of cells for therapy, especially red blood cell products for transfusion (Lapillonne et al., 2010). In concordance with other studies that have aimed to produce red blood cells from feeder-free culture systems (Roy et al., 2012; Smith et al., 2013), all methods analyzed in this study largely reproduced embryonic EMP at developmental stage rather than adult erythropoiesis, with only small (<1%) amounts of β-globin production. This is unlikely to be of clinical value. An alternative approach such as immortalization of early adult erythroblasts, which successfully generated red blood cells with 95% of globin expression of α and β type (Trakarnsanga et al., 2017), may be preferable to current iPSC-based erythropoiesis systems if safety and non-immunogenicity can be confirmed in advanced preclinical models.

In conclusion, our study directly compares four common serum-free, feeder-free approaches for hematopoietic cell production from human iPSCs and demonstrates that an improved 2D-multistep method provides the most robust and efficient method, which is also time- and cost-effective and successfully recapitulates disease phenotypes. This study indicates that investigation into extended Wnt activation and AhR modulation on hematopoiesis using this 2D-multistep method would contribute to a greater understanding of precise control during iPSC hematopoietic differentiation and the capacity for various modifications to recapitulate different stages of normal and aberrant hematopoietic development. Additional optimization, such as novel culture additives and/or genome-engineering approaches, may allow the generation of adult erythropoiesis for production of red blood cells for human transfusion. Finally, this study advocates for direct comparative reporting of iPSC hematopoietic differentiation methods. This facilitates stepwise modifications and improvement of methods to produce target cell populations to most precisely recapitulate or elucidate biological models. Standardization of optimized iPSC hematopoietic differentiation

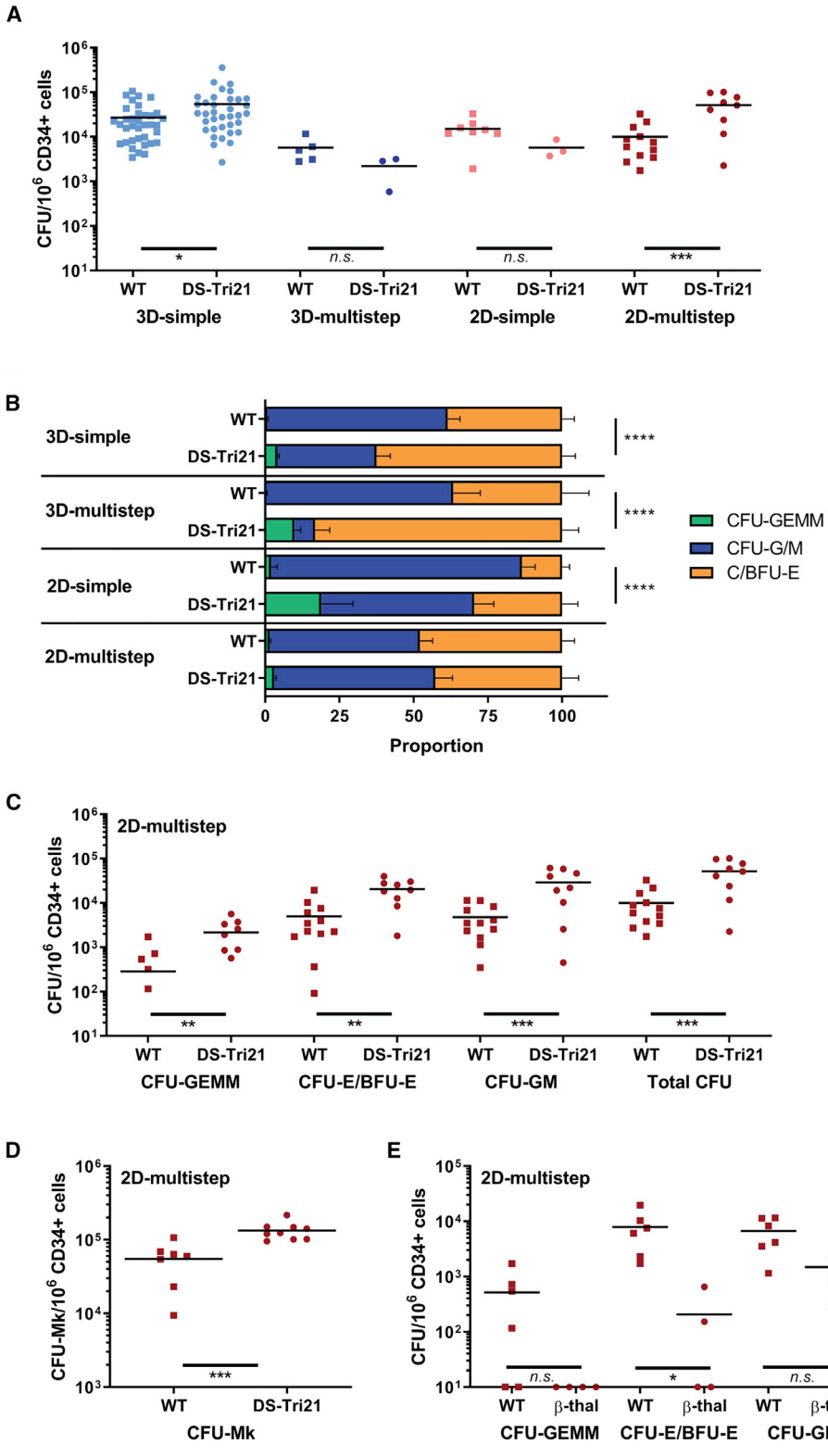

(legend on next page)

would increase versatility and sensitivity of iPSC-based models for medical research and future therapeutic use.

EXPERIMENTAL PROCEDURES

Cell Culture

iPSC lines were generated from WT, DS, or β-thalassemia human fibroblasts using an episomal non-integrating vector as previously reported (Briggs et al., 2013) with the informed consent of patients. Refer to Supplemental Information for more details.

Hematopoietic Differentiation of iPSCs

Refer to Supplemental Information for more details.

The EB simple-step differentiation (3D-simple) method was from Lapillonne et al., (2010), and the EB multistep (3D-multistep) method was from Chou et al., (2012). The monolayer simple differentiation (2D-simple) method was from Niwa et al., (2011). Selection of harvest time points was based on the original publications.

The monolayer multistep (2D-multistep) differentiation method was adapted from Smith et al., (2013) with additional optimization to approximately halve the overall cost of culture reagents and reduce hands-on time by 40%. Some full media changes were altered to media supplementation or were skipped. Cultures were harvested on days 9, 12, 16, and 19 for time-course studies, with suspension cells and dissociated adherent cells analyzed separately. The optimum time point selected was day 16, based on peak CFU frequency. For all other 2D-multistep data the suspension cells alone were used, due to the robust cellular production and higher percentages of hematopoietic cells.

Calculation of Number of Cells or CFU Produced from 1×10^6 iPSCs

Calculations of the number of cells or CFU produced from 1×10^6 iPSCs were calculated from the average number of iPSCs plated per dish per experiment, estimated according to previous experience with iPSC colony size and cell counts.

Clonogenic Colony-Forming Assay

Harvested cells were grown in Methocult Enriched medium (H4435) and Megacult-C medium (04973, Stem Cell Technologies) as per manufacturer's instructions. Refer to Supplemental Information for more details.

OP9 Erythroid Differentiation

2D-multistep day-16 suspension cells were seeded at 50,000 cells per well onto confluent OP9 cell feeder cells and cultured for 17 days with half-volume media changes every 3–4 days. See Supplemental Information for more details.

Flow-Cytometric Analysis

Cells were resuspended in FACS buffer (2% BSA, 0.2% sodium azide, Dulbecco's PBS) and stained with a multicolor panel of conjugated human antibodies. Samples were acquired using a BD LSRII (FacsDIVA 4.0) or BD LSRFortessa X-20 (FACSDiva 8.0), and analyzed by FACSDiva (8.0.1) or FlowJo (10.2). See Supplemental Information for more details.

Quantitative PCR

Total RNA was used to generate cDNA, and qPCR was performed using the Rotor-Gene Q real-time PCR cycler (Qiagen). Data was analyzed with Rotor-Gene 6 Software (Qiagen) for relative gene expression normalized to housekeeping genes (HPRT, GAPDH, and ABL). See Supplemental Information for more details.

Relative Cost

Cost was calculated based on the 2018 list price in US dollars and volume required for all reagents per well of culture, adjusted by the average number of $CD34^+$ cells and CFU produced per method to determine the number of wells required to produce 1×10^6 target cells, shown relative to the cost for the 2D-multistep method.

Hands-On Time

See Supplemental Information for more details.

Figure 4. Comparison of Methods for the Study of Normal and Aberrant Hematopoiesis

(A) The 3D-simple and 2D-multistep methods of iPSC hematopoietic differentiation resulted in increased total CFU per 10^6 $CD34^+$ cells derived from iPSCs from DS individuals compared with wild-type (WT) individuals (2–6 WT iPSC lines, n = 5–36 replicates; 2 DS-Tri21-derived iPSC lines, n = 3–36 replicates; mean indicated by a horizontal line).

(B) When each type of CFU is analyzed as a percentage of total CFU to determine lineage bias, the 3D-simple, 3D-multistep, and 2D-simple methods recapitulated increased proportions of erythroid CFU from DS individuals in comparison with WT individuals (2–9 WT iPSC lines, n = 2–36 replicates; 2 DS-Tri21-derived, n = 4–36 replicates). Mean with standard error of the mean shown.

(C and D) Number of CFU generated using the 2D-multistep method from 10^6 $CD34^+$ progenitor cells was greater for all CFU types from DS than from WT human subjects in Methocult Enriched medium (2 WT iPSC lines, n = 5–12 replicates; 1 DS iPSC line, n = 8–9 replicates) (C) and Megacult-C medium (1 WT iPSC line, n = 7 replicates; 1 DS iPSC line, n = 9 replicates) (D).

(E) Number of CFU generated using the 2D-multistep method from 10^6 $CD34^+$ progenitor cells derived from WT or β-thalassemia human subjects shows the decreased erythroid CFU and total CFU consistent with recapitulation of the β-thalassemia phenotype (1 WT iPSC line, n = 6 replicates; 3 β-thalassemia-derived iPSC lines, n = 4 replicates).

Each point of data indicates an independent replicate with mean indicated by a horizontal line. Statistical significance by t tests are indicated below graphs, with bars positioned to indicate the methods compared (*$p < 0.05$; **$p < 0.01$, ***$p < 0.001$; ****$p < 0.0001$). β-thal, β-thalassemia; BFU-E, burst-forming unit—erythrocyte; CFU-E, colony-forming unit—erythrocyte; CFU-GEMM, colony-forming unit—granulocyte-erythrocyte-monocyte-macrophage; CFU-GM, colony-forming unit—granulocyte and/or macrophage; Total CFU, total colony-forming units from culture in Methocult Enriched medium; CFU-Mk, colony-forming unit—megakaryocyte from culture in Megacult medium; DS, Down syndrome; n.s., not significant; WT, wild type. See also Figure S4.

Statistical Analysis

Statistical analysis was performed using GraphPad Prism 7 (GraphPad Software, San Diego, CA, USA). Ordinary one-way ANOVA with post hoc Tukey's test was used for analyses of multiple groups (incorporating the extension of the Tukey post hoc test, the Tukey-Kramer test, to allow for unequal sample sizes), and unpaired t tests were used to compare individual groups. Chi-squared analysis was used for comparison of CFU proportions between WT and aberrant hematopoiesis. A p value of <0.05 was considered statistically significant.

SUPPLEMENTAL INFORMATION

Supplemental Information can be found online at https://doi.org/10.1016/j.stemcr.2020.07.009.

AUTHOR CONTRIBUTIONS

Conceptualization, M.L.T., T.H.L., H.T., T.J.M., and D.D.M.; Methodology, M.L.T., T.H.L., C.M.A., S.A., E.J.W., H.T., and D.D.M.; Validation, M.L.T., T.J.M., and D.D.M.; Formal Analysis, M.L.T., T.H.L., E.J.W., H.T., T.J.M., and D.D.M.; Investigation, M.L.T., T.H.L., and C.M.A.; Resources, S.A., E.J.W., T.J.M., and D.D.M.; Writing – Original Draft, M.L.T., T.H.L., C.M.A., T.J.M., and D.D.M.; Writing – Review & Editing, M.L.T., T.H.L., C.M.A., E.J.W., H.T., T.J.M., and D.D.M.; Visualization, M.L.T., T.J.M., and D.D.M.; Supervision, M.L.T., T.J.M., and D.D.M.; Project Administration, D.D.M.; Funding Acquisition, M.L.T., T.J.M., and D.D.M.

ACKNOWLEDGMENTS

The authors acknowledge funding support from Arrow Bone Marrow Transplant Foundation, St. Vincent's Clinic Foundation, St. Vincent's Hospital Sydney Hematology Department Research Funds, and statistical advice from Dr Zhixin Liu. The authors declare no competing interests.

Received: April 28, 2020
Revised: July 9, 2020
Accepted: July 9, 2020
Published: August 6, 2020

REFERENCES

Angelos, M.G., and Kaufman, D.S. (2018). Advances in the role of the aryl hydrocarbon receptor to regulate early hematopoietic development. Curr. Opin. Hematol. *25*, 273–278.

Angelos, M.G., Ruh, P.N., Webber, B.R., Blum, R.H., Ryan, C.D., Bendzick, L., Shim, S., Yingst, A.M., Tufa, D.M., Verneris, M.R., et al. (2017). Aryl hydrocarbon receptor inhibition promotes hematolymphoid development from human pluripotent stem cells. Blood *129*, 3428–3439.

Banno, K., Omori, S., Hirata, K., Nawa, N., Nakagawa, N., Nishimura, K., Ohtaka, M., Nakanishi, M., Sakuma, T., Yamamoto, T., et al. (2016). Systematic cellular disease models reveal synergistic interaction of trisomy 21 and GATA1 mutations in hematopoietic abnormalities. Cell Rep. *15*, 1228–1241.

Barouki, R., Aggerbeck, M., Aggerbeck, L., and Coumoul, X. (2012). The aryl hydrocarbon receptor system. Drug Metabol. Drug Interact. *27*, 3–8.

Belay, E., Miller, C.P., Kortum, A.N., Torok-Storb, B., Blau, C.A., and Emery, D.W. (2015). A hyperactive Mpl-based cell growth switch drives macrophage-associated erythropoiesis through an erythroid-megakaryocytic precursor. Blood *125*, 1025–1033.

Bernecker, C., Ackermann, M., Lachmann, N., Rohrhofer, L., Zaehres, H., Arauzo-Bravo, M.J., van den Akker, E., Schlenke, P., and Dorn, I. (2019). Enhanced ex vivo generation of erythroid cells from human induced pluripotent stem cells in a simplified cell culture system with low cytokine support. Stem Cells Dev. *28*, 1540–1551.

Briggs, J.A., Sun, J., Shepherd, J., Ovchinnikov, D.A., Chung, T.L., Nayler, S.P., Kao, L.P., Morrow, C.A., Thakar, N.Y., Soo, S.Y., et al. (2013). Integration-free induced pluripotent stem cells model genetic and neural developmental features of down syndrome etiology. Stem Cells *31*, 467–478.

Carlin, S.M., Ma, D.D., and Moore, J.J. (2013). T-cell potential of human adult and cord blood hemopoietic stem cells expanded with the use of aryl hydrocarbon receptor antagonists. Cytotherapy *15*, 224–230.

Chiang, J.C., Jiang, J., Newburger, P.E., and Lawrence, J.B. (2018). Trisomy silencing by XIST normalizes Down syndrome cell pathogenesis demonstrated for hematopoietic defects in vitro. Nat. Commun. *9*, 5180.

Chou, S.T., Byrska-Bishop, M., Tober, J.M., Yao, Y., Vandorn, D., Opalinska, J.B., Mills, J.A., Choi, J.K., Speck, N.A., Gadue, P., et al. (2012). Trisomy 21-associated defects in human primitive hematopoiesis revealed through induced pluripotent stem cells. Proc. Natl. Acad. Sci. U S A *109*, 17573–17578.

Ditadi, A., and Sturgeon, C.M. (2016). Directed differentiation of definitive hemogenic endothelium and hematopoietic progenitors from human pluripotent stem cells. Methods *101*, 65–72.

Donada, A., Balayn, N., Sliwa, D., Lordier, L., Ceglia, V., Baschieri, F., Goizet, C., Favier, R., Tosca, L., Tachdjian, G., et al. (2019). Disrupted filamin A/alphaIIbbeta3 interaction induces macrothrombocytopenia by increasing RhoA activity. Blood *133*, 1778–1788.

Finotti, A., and Gambari, R. (2014). Recent trends for novel options in experimental biological therapy of beta-thalassemia. Expert Opin. Biol. Ther. *14*, 1443–1454.

Garcia-Alegria, E., Menegatti, S., Fadlullah, M.Z.H., Menendez, P., Lacaud, G., and Kouskoff, V. (2018). Early human hemogenic endothelium generates primitive and definitive hematopoiesis in vitro. Stem Cell Reports *11*, 1061–1074.

Georgomanoli, M., and Papapetrou, E.P. (2019). Modeling blood diseases with human induced pluripotent stem cells. Dis. Model Mech. *12*, dmm039321.

Hansen, M., Varga, E., Aarts, C., Wust, T., Kuijpers, T., von Lindern, M., and van den Akker, E. (2018). Efficient production of erythroid, megakaryocytic and myeloid cells, using single cell-derived iPSC colony differentiation. Stem Cell Res. *29*, 232–244.

Hansen, M., von Lindern, M., van den Akker, E., and Varga, E. (2019). Human-induced pluripotent stem cell-derived blood products: state of the art and future directions. FEBS Lett. *593*, 3288–3303.

Kotini, A.G., Chang, C.J., Chow, A., Yuan, H., Ho, T.C., Wang, T., Vora, S., Solovyov, A., Husser, C., Olszewska, M., et al. (2017). Stage-specific human induced pluripotent stem cells map the progression of myeloid transformation to transplantable leukemia. Cell Stem Cell *20*, 315–328.e7.

Kyttala, A., Moraghebi, R., Valensisi, C., Kettunen, J., Andrus, C., Pasumarthy, K.K., Nakanishi, M., Nishimura, K., Ohtaka, M., Weltner, J., et al. (2016). Genetic variability overrides the impact of parental cell type and determines iPSC differentiation potential. Stem Cell Reports *6*, 200–212.

Lapillonne, H., Kobari, L., Mazurier, C., Tropel, P., Giarratana, M.C., Zanella-Cleon, I., Kiger, L., Wattenhofer-Donze, M., Puccio, H., Hebert, N., et al. (2010). Red blood cell generation from human induced pluripotent stem cells: perspectives for transfusion medicine. Haematologica *95*, 1651–1659.

Lee, J., Dykstra, B., Spencer, J.A., Kenney, L.L., Greiner, D.L., Shultz, L.D., Brehm, M.A., Lin, C.P., Sackstein, R., and Rossi, D.J. (2017). mRNA-mediated glycoengineering ameliorates deficient homing of human stem cell-derived hematopoietic progenitors. J. Clin. Invest. *127*, 2433–2437.

Leung, A., Zulick, E., Skvir, N., Vanuytsel, K., Morrison, T.A., Naing, Z.H., Wang, Z., Dai, Y., Chui, D.H.K., Steinberg, M.H., et al. (2018). Notch and aryl hydrocarbon receptor signaling impact definitive hematopoiesis from human pluripotent stem cells. Stem Cells *36*, 1004–1019.

Liu, G., David, B.T., Trawczynski, M., and Fessler, R.G. (2019). Advances in pluripotent stem cells: history, mechanisms, technologies, and applications. Stem Cell Rev. Rep. *16*, 3–32.

McGrath, K.E., Frame, J.M., Fromm, G.J., Koniski, A.D., Kingsley, P.D., Little, J., Bulger, M., and Palis, J. (2011). A transient definitive erythroid lineage with unique regulation of the beta-globin locus in the mammalian embryo. Blood *117*, 4600–4608.

Mori, Y., Chen, J.Y., Pluvinage, J.V., Seita, J., and Weissman, I.L. (2015). Prospective isolation of human erythroid lineage-committed progenitors. Proc. Natl. Acad. Sci. U S A *112*, 9638–9643.

Ng, E.S., Davis, R., Stanley, E.G., and Elefanty, A.G. (2008). A protocol describing the use of a recombinant protein-based, animal product-free medium (APEL) for human embryonic stem cell differentiation as spin embryoid bodies. Nat. Protoc. *3*, 768–776.

Nishizawa, M., Chonabayashi, K., Nomura, M., Tanaka, A., Nakamura, M., Inagaki, A., Nishikawa, M., Takei, I., Oishi, A., Tanabe, K., et al. (2016). Epigenetic variation between human induced pluripotent stem cell lines is an indicator of differentiation capacity. Cell Stem Cell *19*, 341–354.

Niwa, A., Heike, T., Umeda, K., Oshima, K., Kato, I., Sakai, H., Suemori, H., Nakahata, T., and Saito, M.K. (2011). A novel serum-free monolayer culture for orderly hematopoietic differentiation of human pluripotent cells via mesodermal progenitors. PLoS One *6*, e22261.

Papapetrou, E.P. (2019). Modeling myeloid malignancies with patient-derived iPSCs. Exp. Hematol. *71*, 77–84.

Razaq, M.A., Taylor, S., Roberts, D.J., and Carpenter, L. (2017). A molecular roadmap of definitive erythropoiesis from human induced pluripotent stem cells. Br. J. Haematol. *176*, 971–983.

Reid, J.C., Tanasijevic, B., Golubeva, D., Boyd, A.L., Porras, D.P., Collins, T.J., and Bhatia, M. (2018). CXCL12/CXCR4 signaling enhances human PSC-derived hematopoietic progenitor function and overcomes early in vivo transplantation failure. Stem Cell Reports *10*, 1625–1641.

Roy, A., Roberts, I., Norton, A., and Vyas, P. (2009). Acute megakaryoblastic leukaemia (AMKL) and transient myeloproliferative disorder (TMD) in Down syndrome: a multi-step model of myeloid leukaemogenesis. Br. J. Haematol. *147*, 3–12.

Roy, A., Cowan, G., Mead, A.J., Filippi, S., Bohn, G., Chaidos, A., Tunstall, O., Chan, J.K., Choolani, M., Bennett, P., et al. (2012). Perturbation of fetal liver hematopoietic stem and progenitor cell development by trisomy 21. Proc. Natl. Acad. Sci. U S A *109*, 17579–17584.

Salomonis, N., Dexheimer, P.J., Omberg, L., Schroll, R., Bush, S., Huo, J., Schriml, L., Ho Sui, S., Keddache, M., Mayhew, C., et al. (2016). Integrated genomic analysis of diverse induced pluripotent stem cells from the Progenitor Cell Biology Consortium. Stem Cell Reports *7*, 110–125.

Smith, B.W., Rozelle, S.S., Leung, A., Ubellacker, J., Parks, A., Nah, S.K., French, D., Gadue, P., Monti, S., Chui, D.H., et al. (2013). The aryl hydrocarbon receptor directs hematopoietic progenitor cell expansion and differentiation. Blood *122*, 376–385.

Trakarnsanga, K., Griffiths, R.E., Wilson, M.C., Blair, A., Satchwell, T.J., Meinders, M., Cogan, N., Kupzig, S., Kurita, R., Nakamura, Y., et al. (2017). An immortalized adult human erythroid line facilitates sustainable and scalable generation of functional red cells. Nat. Commun. *8*, 14750.

Wattanapanitch, M., Damkham, N., Potirat, P., Trakarnsanga, K., Janan, M., U-Pratya, Y., Kheolamai, P., Klincumhom, N., and Issaragrisil, S. (2018). One-step genetic correction of hemoglobin E/beta-thalassemia patient-derived iPSCs by the CRISPR/Cas9 system. Stem Cell Res. Ther. *9*, 46.